A Multiscale Approach for the Characterization and Crystallization of Eflucimibe Polymorphs: from Molecules to Particles

Sébastien Teychené, Béatrice Biscans

A Multiscale Approach for the Characterization and Crystallization of Eflucimibe Polymorphs: from Molecules to Particles †

S. Teychené and B. Biscans
Laboratoire de Génie Chimique UMR CNRS 5503, Université de Toulouse[1]

Abstract

We present in this paper a generic multiscale methodology for the characterization and crystallization of eflucimibe polymorphs. The various characterization techniques used have shown that eflucimibe polymorphism is due to a conformational change of the molecule in the crystal lattice. In addition, the two polymorphs are monotropically related in the temperature range tested and have similar structures and properties (ie. interfacial tension and solubility). Consequently, it was found that for a wide range of operating conditions, the polymorphs may crystallize concomitantly. Induction time measurements and metstable zone width determination allow to infer the origin of the concomitant appearance of the polymorphs. A predominance diagram has been established which allows to perfectly control the crystallization of the desired polymorph. However, even if the stable form can be produced in a reliable way, the crystal suspension went toward a very structured gel-like network which limits the extrapolation process. Based on microscopic observation of the crystallization events performed in a microfluidic crystallizer, we propose a range of operating conditions suitable for the production of the stable form with the desired handling properties.

Keywords: Crystallization, Rheology, microfluidic, Polymorphism, Nucleation

Introduction

Crystallization from solution is a core technology in pharmaceutical industries. Usually, this process is a part of a wide processing system, including solid–liquid separation, particle design, and formulation. Chemical engineers must develop a robust crystallization process that delivers the active pharmaceutical ingredient (API) with both high yield and appropriate attributes that are conducive to drug product development (e.g., purity, polymorph and particle size distribution). Crystal polymorphism, which has been extensively studied in the past ten years, is the ability of a molecule to crystallize as more than one distinct crystal phases that have different arrangement and/or conformation of the molecule in the crystal lattice. Polymorphism of drug substances is very common and concerns about 90% of small organic molecules (Lipinsky 2001, Griesser 2003). It influences every aspect of the solid-state properties of a drug. It also leads to dramatic effects in biological activity between two forms of the same drug. The most important consequences of polymorphism in pharmaceuticals are the possibility of conversion among polymorphic forms and the variation in bioavailability of the drug substances. In addition to these constraints the crystallization process have to be designed to produce crystals with good handling properties which can be very tricky when dealing with complex and flexible molecules that crystallize only as needles or fibers (i.e. particles with aspect ratio greater than 10). The aim of this paper is to present characterization measurements, at multiscales and process design of a complex molecule, eflucimibe (S)-2',3',5'-trimethyl-4'-hydroxy-α-docecyl acetanilide, a new acyl-coenzyme A-cholesterol O-acyltransferase (ACAT) inhibitor developed by Pierre Fabre Research Centre. The first part of the paper is dedicated to the solid-state characterization of the different polymorphs of eflucimibe using a combination of different analytical techniques (XRPD, Raman spectroscopy, MNR spectroscopy and

† Accepted : September 16th, 2011
1 4 allée Emile Monso 31432 Toulouse Cedex 4, FRANCE
* Corresponding author
E-mail:sebastien.teychene@ensiacet.fr.
TEL: (+33)534323637 FAX: (+33)34323697

thermal analysis). This approach allows us to determine the thermodynamic relationships between polymorphs and the solid(s) – liquid equilibrium. Then, for designing a robust crystallization process to produce the stable form, the control and the knowledge of the nucleation step from solution is the key parameter. The second part of the paper deals with the determination of nucleation kinetics of eflucimibe, using classical crystallization experiment (i.e. induction time) and by non-classical experiment using a microfluidic crystallizer recently developed. In the final part of the paper, the crystallization process itself is explored. Based on the rheological experiments performed on eflucimibe suspension, we propose a solution for operating the crystallization process to produce in a reliable way the desired polymorph with good handling properties. This paper has been written in order to present a generic methodology from the molecular scale to the crystallization process scale.

1. Solid State Characterization

1.1 X-Ray diffraction patterns

As eflucimibe crystals are weakly diffracting, classical XRPD does not allow the discrimination of the two polymorphs, XRPD patterns were obtained from synchrotron radiation (ESRF Grenoble, France).

The samples were mounted in 1.0mm borosilicate capillaries the diffraction investigations. Wavelength of 0.515529Å was selected using a double Si(111) monochromater. Data were collected at room temperature using a Ge(111) analyzer crystal/NaI scintilliator/PMT detector arrangement, which allows very high angular resolution (<0.003° 2θ). Data were collected between 0.75 and 20° 2θ. Diffraction data upon heating were taken using a 2D detector system (Fiber optic coupled CCD camera) having an angular resolution of 0.02° 2θ in this configuration. This arrangement allows rapid acquisition of diffraction patterns with good counting statistics. Upon heating the angular range covered was 0.7° <° 2θ<15°. Samples were heated in air with 0.3℃ steps from 25℃ to 135° C. After each step, the samples were allowed to equilibrate for 20-30 s, followed by a 5s acquisition time. The temperature stability of the furnace was around 0.1℃

Representative high-resolution diffraction patterns obtained for the two pure phase samples are given in **Fig. 1**.

Both samples are weakly diffracting, display significant peak broadening, and do not scatter at very high angle. Due to the poor crystallinity of the samples, it was not possible to derive even the unit cells from any of the diffraction patterns. The first three diffraction peaks appear to be multiples of a long axis (35Å at room temperature). In addition, these peaks and further multiples (identified as 00L in **Fig. 1**) are sharper than the other peaks, indicating that all belong to the same zone axis ; the narrow width of these peaks indicating a better crystalline order in this direction. The broadening observed in non-00L peaks indicates a greater degree of disorder along the long axis, consistent with the prolate form

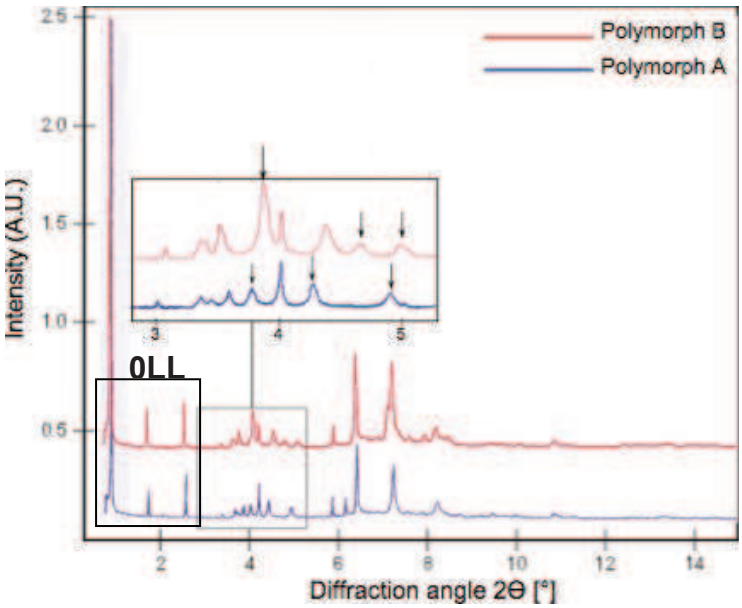

Fig. 1 Synchrotron Powder X-Ray diffraction pattern of Eflucimibe polymorphs.

of the molecule. As the first non-00L peaks appear at smaller d-spacing (<8.2 Å) the other axes appear more shorter. Thus, structures for both phases may be hypothesized in which the molecules are aligned along the long cell axes (d～ 35 Å). This is consistent with the presence of the two aliphatic chains in the cell axes. Different phases would be due to different orientation settings of the molecules about this axis, a typical situation for such organic molecules. An hypothetic structure is given in **Fig. 2**.

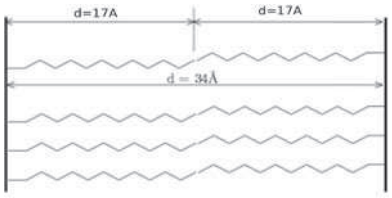

Fig. 2 Molecular arrangement of eflucimibe molecules in the crystal lattice.

Identification of the different polymorphs is performed using the most representative peaks of the two phases. As shown in **Fig. 1**, reasonably well separated peaks belonging only to one of the two polymorphs can be identified in the range 3 to 6° 2θ. Portions of the diffraction patterns collected on heating samples of phases A and B are given in **Fig. 3a** and **3b** respectively. For the A form, a clear 1st order phase transition is obvious, beginning near 110℃. A complex thermal event that extends from 75℃ to 105 ℃ is more subtle and can be attributed to an alteration of the lamellar structure. Melting occurs at 130 ℃.

For form B, two first order transitions are observed, occurring near 75℃ and 110℃. Melting occurs, also, near 130℃. In addition, by comparing the behaviour of both polymorphs under heating, no common diffraction peaks (or phases) were found, i.e. no transition between A and B are observed in the temperature range tested.

Even if single crystal diffraction patterns, and thus the crystal structure, are not available, this study allows us to determine an identification method for discriminating the two eflucimibe polymorphs.

1.2 Thermal analysis

1.2.1 Thermogravimetric analysis (DTA)

Thermogravimetric analysis were performed in a TA 2000 (TA instrument). 15 to 20 mg of eflucimibe crystals were weighted and placed in a platinium furnace under a nitrogen purge (Q=20ml.min^{-1}) and heated from 20 to 450℃ with a heating rate of 5℃ .min^{-1}. For all the samples tested, no mass loss was detected in the temperature range from 25 to 150℃ . For both polymorphs, decomposition occurs at 180 ℃. These results show that there is no solvates and Differential Scanning Calorimetry can be used to study the polymorphism of eflucimibe crystals.

1.2.2 Differential Scanning Calorimetry (DSC)

Thermograms were obtained in a DSC 2920 from TA instrument. 2 to 4mg of the samples were weighted and placed in a sealed aluminium furnace. The sample was then heated from -40 to 140℃ at a constant rate of 5℃.min^{-1} under a nitrogen purge (Q=20ml.min^{-1}). The reversibility of the thermal events observed was checked by performing heating and cooling cycles before melting. Representative thermograms of the A and B forms are given in **Fig. 4**.

All the thermal event observed are consistent with the results obtained from XRPD diffraction patterns. In addition, the phase transition observed at 35℃ is reversible and very fast. As a consequence, only the A1 form (stable form at 35℃) of polymorph A will be considered in this study.

As the results obtained by DSC and XRPD are in good agreement, DSC could be used as a semi-

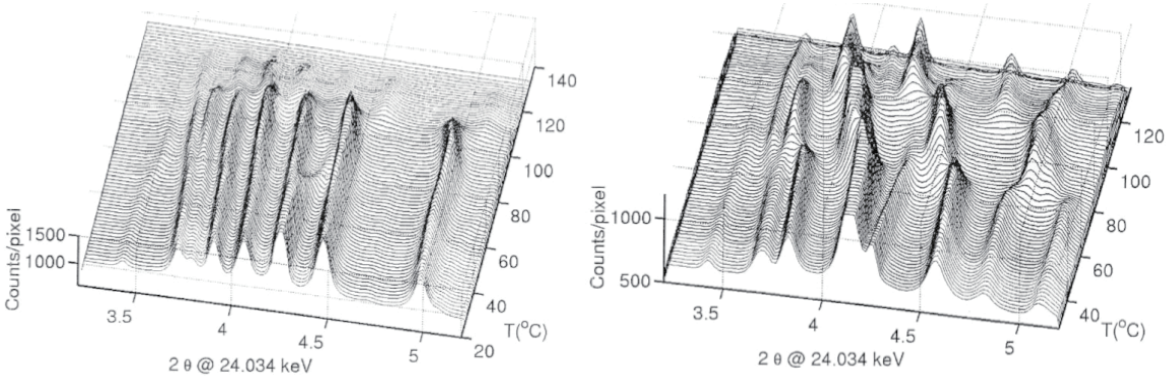

Fig. 3 XRPD diffraction pattern as function of temperature (a) Polymorph A (b) Polymorph B.

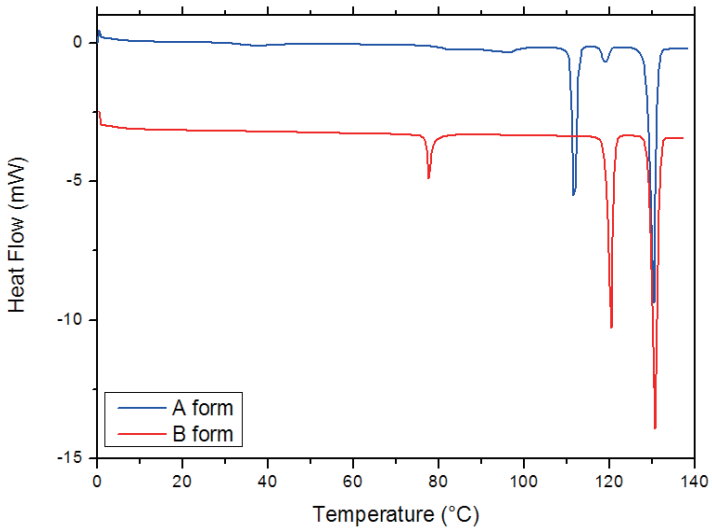

Fig. 4 DSC thermogramms of eflucimibe polymorphs (red: B form, blue: A form).

quantitative method for determining the amount of polymorph in a mixture. The polymorphic composition of the powder is then obtained by the following equation:

$$w_A = \frac{1}{2}\frac{A_{fus}^{ref}}{A_{fus}}\left(\frac{A_{110}}{A_{110}^{ref}} + \frac{A_{35}}{A_{35}^{ref}}\right) \quad (1)$$

Where the superscript *ref* refers to the pure A form, and A_{fus}, A_{110}, A_{35} are the area of the characteristics peaks of the A form at 130℃, 110℃ and 35℃ respectively.

This method has been used to characterize physical mixtures of eflucimibe polymorphs. The results obtained are given in **Table 1**.

The results obtained in **Table 1**, expressed in terms of standard deviation and reproducibility, suggest that this method is at most semi quantitative, and can be used to know precisely if pure A or B polymorph is obtained.

1.3 Spectroscopic analysis

1.3.1 Solid State CPMAS-MNR Spectroscopy

Eflucimibe ^{1}H and ^{13}CRMN/CP-MAS spectra were obtained with a Bruker DMX-500 spectrometer operating at 125.7 MHz. 50 mg of powder samples were packed into 7mm zirconium rotors and spun at 8 kHz at the magic angle of 54° 44'' . Spectra were acquired using a cross polarization contact time of 500μs, decoupling of 1H is performed during the acquisition of ^{13}C signal.

As shown in **Fig. 5**, the spectra obtained for the two polymorphic forms are similar, which suggests similar arrangement of the molecules in the crystal lattice for the two polymorphs. Attribution of the spectral band of the solid-state ^{13}C MNR spectra are based on the comparison with high resolution MNR spectra of DMSO. Resonance from the three carbons at 168ppm (C-1), 146ppm (C-4') and 22ppm (C-11'') are split in doublets, which indicates that two or four eflucimibe molecules are in the crystal asymmetric unit. The chemical shift of the methyl group between 15 and 5ppm is different from a polymorph to another. This difference could be attributed to a conformational difference of the corresponding benzyl group. These results suggest that the two polymorphs are due to a difference in the conformation of the molecule in the crystal lattice (conformational polymorphism) (Yu et al. 2000). This conclusion is in agreement with FTIR spectroscopy performed in previous study (Teychene et al 2004, Ribet et al. 2001), in which it was found that the main differences between the two polymorphs spectra are due to different intramolecular hydrogen bond involving the -OH group of the molecule.

1.3.2 Raman Spectroscopy

Raman spectra were collected using a Raman microscope (Kaiser Optical Systems, Leica DM1) equipped with a thermoelectrically cooled CCD detector. The source was a 400mW diode laser operating at 785nm, with an average power output of 100 - 200mW through a 20x, 11 mm working distance objective. The spot size of the laser beam through the objective was approximately 20μm. The microscope was coupled to the spectrometer with multi-mode

Table 1 Characterization by DSC of physical mixture of A and B polymorphs

Sample	Mass fraction of A	Calculated mass fraction of A	Standard deviation (mf)	Number of tested samples
1	0.81	0.83	0.2	3
2	0.5	0.54	0.18	4
3	0.33	0.25	0.13	5
4	0.25	0.18	0.1	5

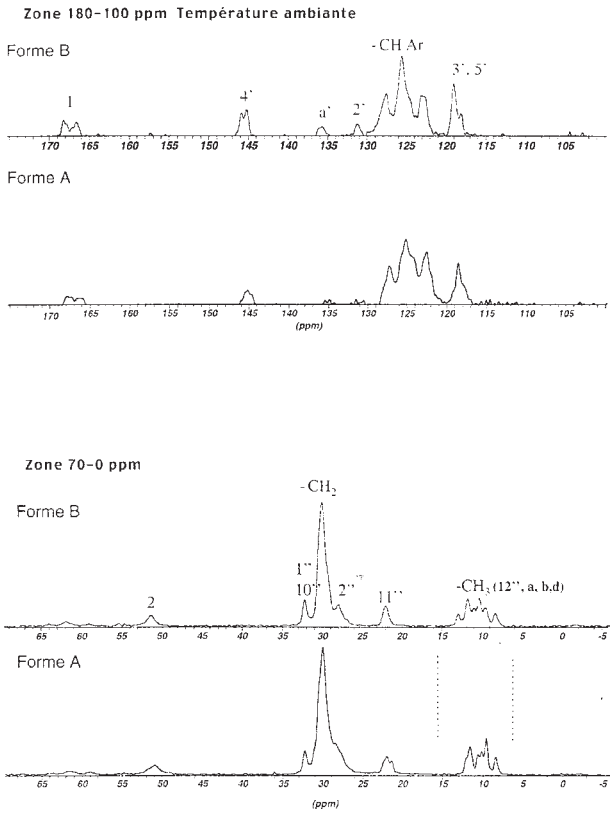

Fig. 5 MNR Spectroscopy of eflucimibe polymorphs (upper trace: B).

fibre optic cables; 50µm diameter was employed for excitation, and 62.5µm diameter for collection. The collection range was 100–3100 cm^{-1}. Raman spectra were collected using approximately 1mg of compound. Samples were placed on a microscope slide, and first focused visually, using a white light source and subsequently re-focused to maximize the Raman signal. An integration time of 1min was used for most samples as this gave good signal-to-noise ratios without damaging the sample.

The Raman spectra obtained for form A and B of eflucimibe are given in **Fig. 6**. The two polymorphs have very similar spectra except for a number of small differences.

In the range of wave number lower than 250 cm^{-1}, no differences in the Raman spectra can be identified, this result suggests that the crystal lattice of the two polymorphs is nearly the same. However, as shown in **Fig. 5**, in the range 1180 – 1210 cm^{-1} form B has a characteristic peak. This peak can be attributed to a change of the vibration mode of the –OH groups involved for example in different hydrogen bond arrangement between the crystalline states. Form B has also characteristic peaks in the range of 600 cm^{-1} and 940-950 cm^{-1}. This peaks are more subtle to interpret but it may be postulated that they may be due to different vibrational mode of the –CH group linked to the aromatic ring.

In that case Raman spectroscopy can be used as a reliable analysis tool for identifing the polymorph nature of the powder. However, it was not possible to achieve a good chemiometric procedure in order to perform quantitative analysis, because mixing of calibration samples and inhomogeneities (due to the

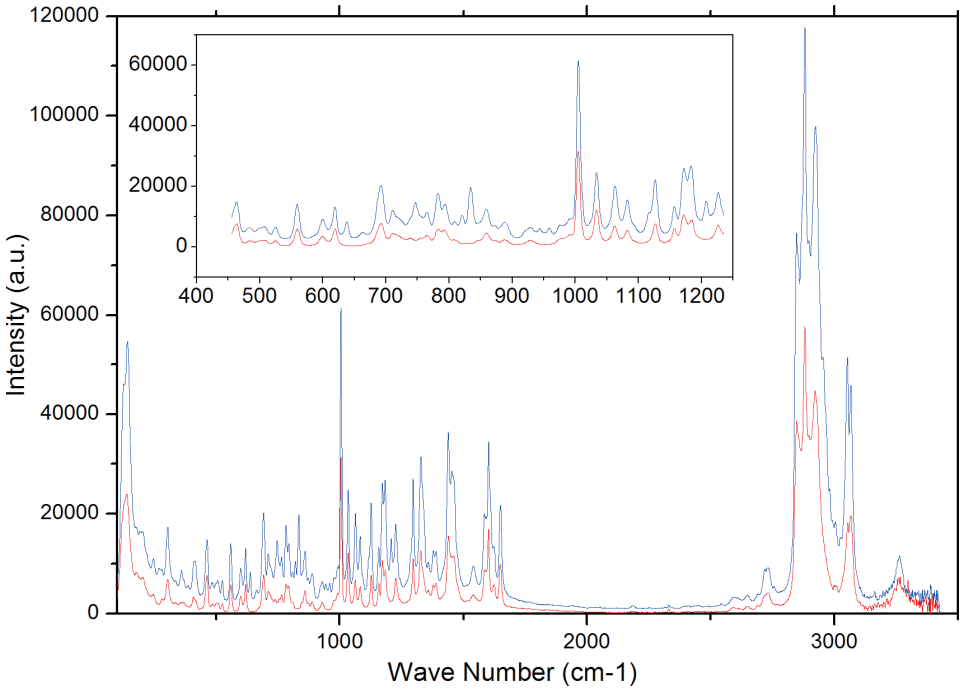

Fig. 6 Raman spectra of A and B polymorphs.

low special resolution of the system (~20μm)) are sources of large experimental errors. In addition, due to the low solubility of eflucimibe in solvents, liquid state analysis is below the detection threshold of the system.

2. Solid Liquid equilibria

2.1 Solubility

In previous study (Teychené et al. 2006), solubility of eflucimibe polymorphs was determined in different solvents and solvents mixtures. The solubility of the two forms is very close in all solvents and temperature tested. From solubility data determined in pure ethanol, it can be stated that in the temperature range of the crystallization process (from 20 to 55℃), the A form has the lowest solubility, and is the thermodynamic most stable polymorph (**Fig. 7a**). In the range of temperature tested, the two polymorphs are monotropically related.

As shown in **Fig. 7b**, in mixtures of ethanol and n-heptane, the solubility profiles of the two polymorphs reach a single maximum. From solvent solubility parameters analysis, it can be stated that, if no solid–solid transition occurs during solubility measurements, the solubility enhancement obtained in solvent mixture is explained in terms of enthalpy–entropy relationships. The entropic gain from loss of ethanol structure (due to the non-polar part of the molecule) is responsible, at first, for the solubility increase. Above a certain concentration of co-solvent, the solubility increase is favored by the enthalpy decrease, due to the solvent–solute hydrogen bond formation mainly due to the evolution of solvent–solute polar interactions. (Domanska 1989, Bustamante et al. 2002).

Several thermodynamic models were tested for the prediction of solubility in ethanol/n-heptane mixtures. The prediction of solubility by using the UNIQUAC equation, with interaction parameters for binary solvent mixture taken from vapour liquid equilibrium, gives satisfactory results. This model describes well ($P^2 > 0.97$) the solubility curves and the solubility maximum found for each polymorphs experimentally at a solvent ratio Ra = 0.7.

As the UNIQUAC model considers the energetic contribution of the crystal form in the solubility calculations, it is highly useful for predicting the polymorphs solubility in solvents mixtures even though the polymorphs properties are very close.

2.2 Phase transition experiments

To ensure that the A form is the stable one, ripening experiments were performed. In these experiments weighted quantity of both pure polymorphs were placed in an ethanol-heptane mixture (Ra=0.7) in an hermetically sealed vessel under slow mixing rate at ambient temperature for four days. Samples

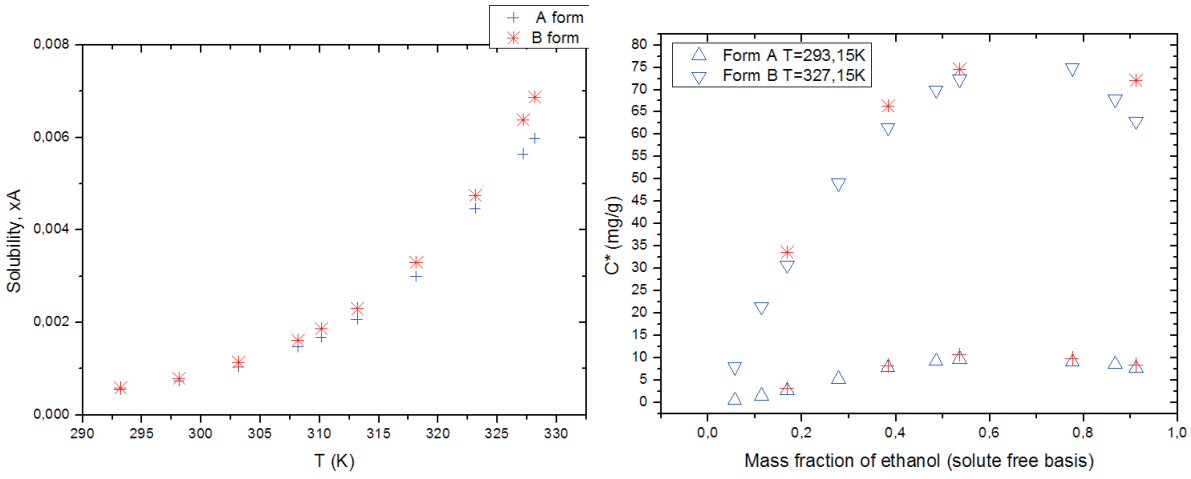

Fig. 7 Solubility of eflucimibe polymorphs in (a) pure ethanol (b) ethanol / n-heptane mixtures.

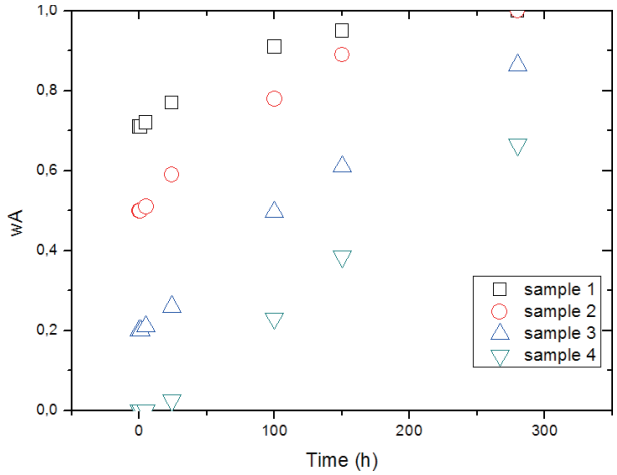

Fig. 8 Evolution in solution of polymorph composition at 300K.

were withdrawn at fixed time intervals. The polymorph composition of the powder was assessed by DSC. The operating conditions and the results obtained in terms of polymorph composition are given in **Fig. 8**.

This figure clearly show that in solution, even if the experimental results are tainted with an experimental error of about 20% due to the analytical technique used (DSC), form B slowly evolves to form A. This result is in agreement with the fact that the A form is the stable one. In addition, from a process point of view, due to the low A to B kinetic transition, it seems unreasonable to perform a maturation step after the crystallization process to obtain pure A form.

3. Nucleation and metastable zone width.

The main objective of eflucimibe crystallization process is to produce the stable form A. As a general rule, the stable polymorph of a drug is produced to ensure constant solid-state properties of the molecule during the whole life of the drug. Producing the stable form avoids unwanted solid-to-solid transitions during handling, storage and formulation. In addition, due to the similar structure of the two polymorphs and their low solubility differences, the metastable form does not increase bioavailability compared to the stable one. Considering that the transition from the metastable to the stable form of eflucimibe is very slow, the production of the stable form of the drug has to be controlled by the crystallization process. As the initial step of crystallization, nucleation is the key

factor for controlling the appearance of the desired polymorph (Ulrich et al. 2002). Nucleation of eflucimibe polymorphs has been extensively studied in previously published papers (Teychené et al. 2004). In these previous papers, the metastable zone widths of eflucimibe were determined in a stirred reactor in ethanol and n-heptane mixtures. The operating conditions tested were the initial concentration, the temperature, the mixing rate, the cooling rate, and the amount of seed introduced during the process. It was found that when crystallization is performed without seeding, for most of the operating conditions tested, both polymorphs appear concomitantly. However, at low initial concentration, the A form seems to crystallize preferentially. At higher initial concentration, the reverse is observed.

When seeds of polymorph A are introduced in the crystallizer, at high initial concentration, nucleation of polymorph B cannot be avoided. When the crystallizer is seeded with polymorph B, the B form is always obtained. The unsuccessful seeding procedure may be explained either by the presence of undetected amount of polymorph B in the seeds or by the narrow window of seeding due to the very low solubility difference between the two forms (lower than 2℃ at higher concentration).

The results obtained are summarized in a "polymorph occurrence diagram" given in **Fig. 9**.

To get more detailed information about nucleation, induction time measurements were performed in a stirred tank. In this work, eflucimibe dissolved in ethanol/n-heptane (Ra=0.75) mixture were quenched from different initial temperatures (ranging from 55 ℃ to 37℃) toward 35℃. The induction time was determined by detecting the pour point of the solution.

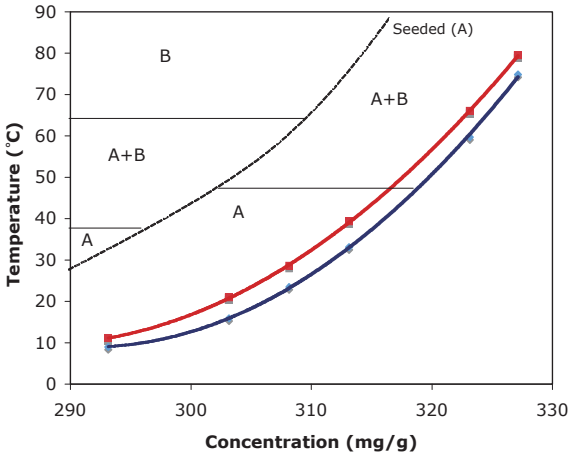

Fig. 9 Occurrence diagram of eflucimibe polymorphs for seeded and unseeded crystallization.

The results presented in Teychene et al. 2008, show that the nature of the nucleating polymorph greatly depends on the supersaturation level of the solution. At high supersaturation, this polymorphic system follows the Ostwald rule of stage. In addition, it was also found that the proportion of nucleating polymorph, in the solid recovered soon after nucleation, is directly linked to the relative nucleation rate of the polymorphs.

From a thermodynamic point of view, by taking the classical nucleation theory, the Gibbs free energy of a nucleating crystal is written as follows (Kashief 1995, Zetttlemoyer 1969):

$$\Delta G_{nucl} = \Delta G_{nucl}^{surf} + \Delta G_{nucl}^{vol} = 4\pi r^2 \gamma_{SL} - \frac{4}{3}\frac{\pi r^3}{v} RT \ln(S) \quad (2)$$

Where r is the diameter of the critical cluster (m), v is the molar volume of the molecule ($m^3.mol^{-1}$) and γ_{SL} ($mJ.m^{-2}$) is the interfacial energy between the nucleus and the saturated solution. The value of γ_{SL} are respectively 5.23 $mJ.m^{-2}$ and 4.17 $mJ.m^{-2}$ for the A and B polymorph, respectively (Teychene et al. 2008). The evolution of the Gibbs free energy during nucleation is given in **Fig. 9a** for a supersaturation ratio of 1.6 and in **Fig. 9b** for S=3.

Fig. 9a and **9b** clearly show that at lower supersaturation, the Gibbs free energy of nucleation is lower for polymorph A than for polymorph B. At higher supersaturation the contrary is observed. This means that, for instance at low supersaturation, the energy barrier for nucleation and the corresponding critical radius are lower for the A form. **Fig. 9c** and **9d** show the evolution of the nucleation barrier (ΔG_{crit}) and of the critical radius as a function of supersaturation. These figures indicate that the trend is reversed for a supersaturation ratio about 1.8. At intermediate supersaturation ratio (from 1.7 to 2), corresponding to the supersaturation range characteristic of the crystallization process, the critical Gibbs free energy and the corresponding critical cluster are nearly the same for both polymorphs, leading to a concomitant appearance of the two polymorphs.

Given the low differences in physico-chemical properties of the two polymorphs, the production of pure polymorph A during a crystallization process can be performed only at low supersaturation level and low temperature. To induce nucleation, and to speed up the crystallization process, A form seeds may be introduced nearly at the equilibrium temperature.

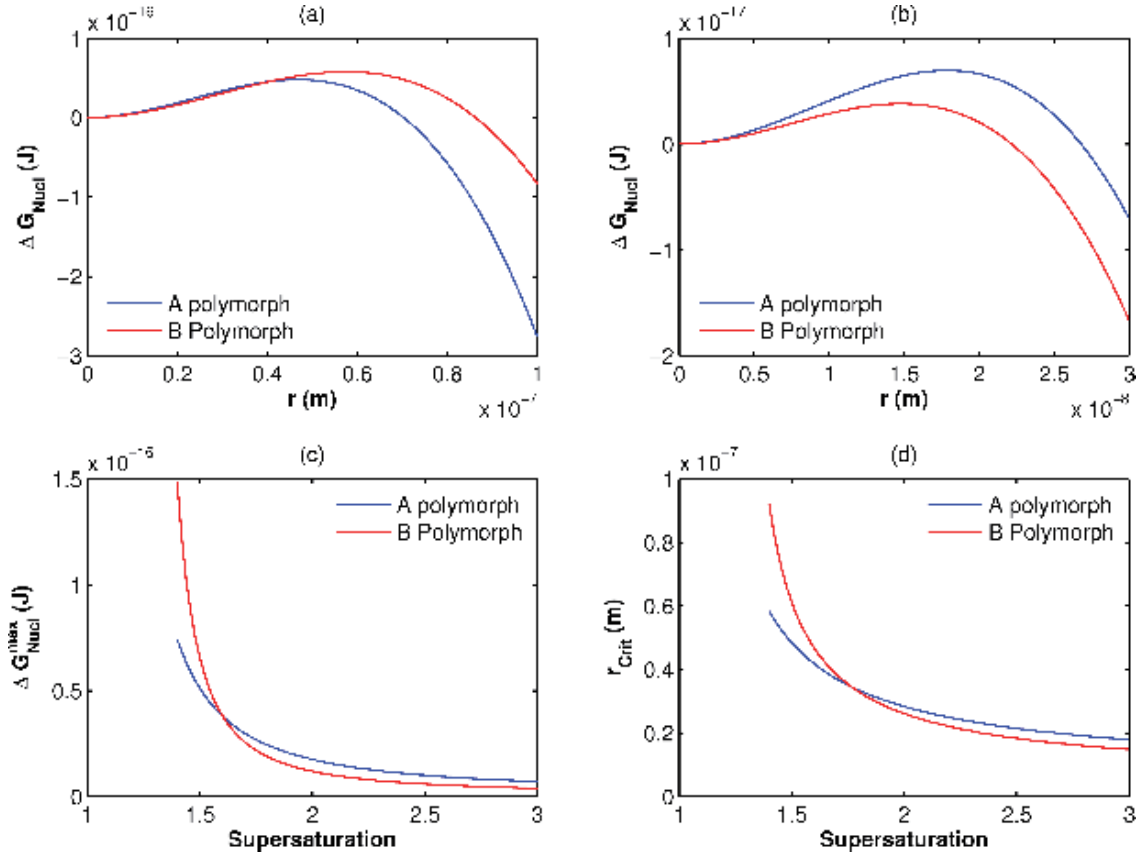

Fig. 10 Evolution of the Gibbs free energy during nucleation (a) and (b) Evolution of the gibbs free energy of nucleation of both polymorphs at S=1.6 and S=3, respectively. (c) Evolution of ΔG_{Nucl}^{Max} vs. Supersaturation. (d) Evolution of the critical radius diameter vs supersaturation.

4. Conventional crystallization process

4.1 Crystallization experiments

Cooling crystallization experiments were carried out in a 1L glass double-jacketed reactor mounted in a Labmax automated system (Mettler Toledo). Mixing is ensured by an A310 propeller from Lightnin (d=6cm). The stirring rate and the corresponding torque were measured during the process. Suspension turbidity was followed during the experiment by a backscattering light probe (FSC 402, Mettler Toledo). Eflucimibe solutions of several concentrations ranging from 82 mg.g^{-1} to 31 mg.g^{-1} in a mixture of ethanol and n-heptane (Ra=0.7) were heated up to 5℃ above the solubility temperature and then cooled down to 20℃ at a constant cooling rate (from 5 to 20℃.h^{-1}). Activated seeds of polymorph A were introduced when saturation temperature of form A was reached. The obtained suspension were either sampled and characterized by rheology or filtered and slowly dried and analyzed by DSC, XRPD, and SEM.

Whatever the operating conditions are, the results obtained in terms of polymorph composition at the end of the process are in good agreement with the results previously obtained in nucleation and metastable zone width experiments. The occurrence diagrams are neither influenced by the stirring rate nor cooling rate, nor scale-up. For instance, the evolution of the polymorph composition of the crystals during the process are given in **Table 2** for a cooling rate of 10℃.h^{-1} and a stirring rate of 200 rpm and for different initial concentrations.

Even if the polymorph purity of eflucimibe crystals can be handled during the crystallization process, handling properties of the suspension obtained at the end of the process is still difficult. Indeed, soon after the nucleation step the system evolves trough a very structured gel-like network that induces a jamming of the suspension. The evolution of the suspension in the reactor is shown in **Fig. 11**.

The evolution of turbidity during the crystallization process for four initial concentrations is given in **Fig. 12**. These results clearly show that for initial concentration above 31mg.g^{-1}, after the introduction of the seeds in the crystallizer, turbidity increases quickly

Table 2 Evolution of polymorph composition and crystallization yield during the seeded crystallization process of eflucimibe

C° (mg.g-1)	T (℃)	Yield (%)	WA (DSC)
81.79	326.5	2%	0.75
	325.3	10%	0.65
	324.7	17%	0.53
	320.5	37%	0.33
	318.9	42%	0.18
	317.2	49%	0.15
	315.5	56%	0.13
	307.7	74%	0.11
	298.2	87%	0.11
59.69	319.9	4%	0.70
	318.3	18%	0.64
	317.1	36%	0.56
	315.9	36%	0.47
	314.8	40%	0.41
	307.3	62%	0.31
	304.4	69%	0.30
	295.3	82%	0.27
43.53	316.3	2%	0.95
	315.0	7%	0.96
	313.6	16%	0.97
	302.8	63%	0.98
	298.3	72%	0.98
31.74	312.1	0%	1.00
	310.9	4%	1.00
	309.6	14%	1.00
	295.2	68%	1.00
	286.1	68%	1.00

and reaches a plateau around NTU =65 -70% before the end of the crystallization process. The turbidity plateau is due to the jamming of the reactor, dense agglomerates are formed around the turbidity probe, the optical thickness of the suspension is increased inducing saturation of the turbidity signal. From this point, the turbidity sensor gives only information about the surrounding agglomerates and not on the overall suspension in the crystallizer.

The volume fraction of solid, obtained by sampling the suspension during the crystallization process, corresponding to the gelation threshold is around 2% at 23℃ and 5% at 40℃ . In **Fig. 12** photographs of dried powder are shown. For the whole operating conditions tested, needle like crystal are obtained with width around 200nm and length ranging from 10 to 30μm.

4.2 Characterization by rheology

As all the classical characterization techniques (BET surface area, Laser diffraction, Back scattering light...) failed to describe the structural evolution of the suspension during the crystallization process, suspensions where characterized by rheology. During these experiments, evolutions of the elastic modulus and the yield stress were recorded as a function of the shear rate or strain for different solid volume fractions. By taking the assumption that the elementary particles, that are responsible for the suspension gel-like structure have a spherical shape, The yield stress and the macroscopic elastic modulus of the network are function of the state of aggregating particles, characterized by the fractal dimension and of the mechanical properties of the particles making up the network. This approach relies on the assumption that the primary particles, responsible

(a) (b) (c) (d)

Fig. 11 Evolution of the crystal suspension during the crystallization process (a-b) nucleation and crystal growth: formation of the suspension (c) Suspension thickening (d) Crystallizer jamming.

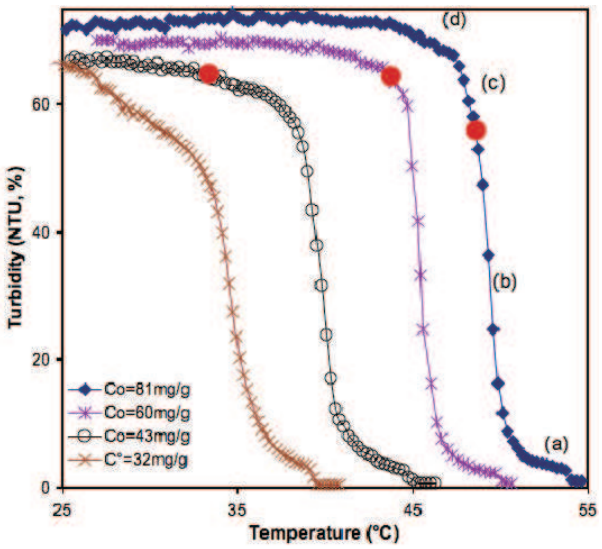

Fig. 12 Evolution of solution tubidity during the crystallization process. The letters (from a to b) correspond to the photographs shown in **Fig. 11**.

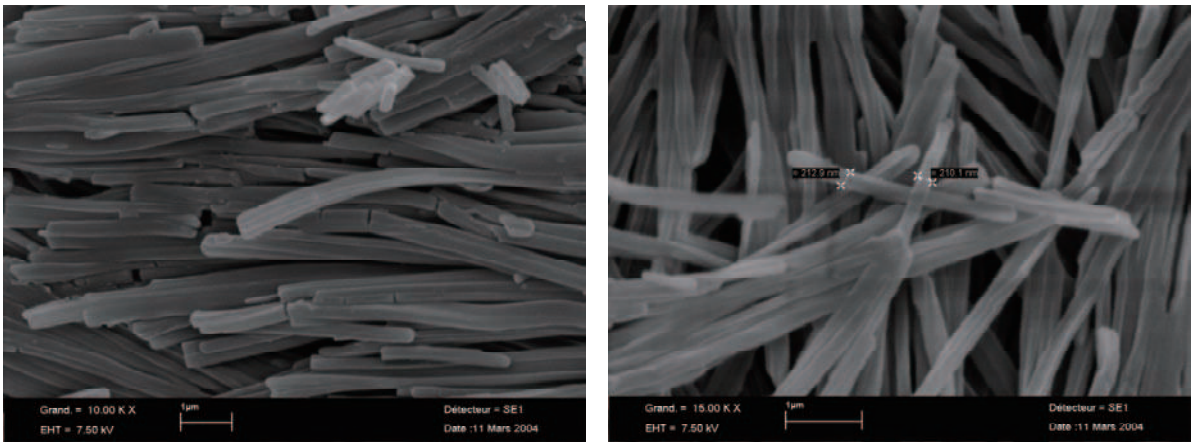

Fig. 13 MEB photomicrographs of eflucimibe crystals obtained at the end of the process.

of the suspension gel-like behavior, have a spherical shape. Knowledge of the fractal dimension as well as the dependence of the rheological properties of the particles with the particle volume fraction are used to infer the mechanism by which the network was formed. (Brown et al. 1985, Buscall 1988) .

Suspension rheology experiments were performed in simple shear and oscillatory mode at 298K in a Bohlin rheometer equipped with parallel-grooved plates (gap=1.2mm, d=2.5mm) to avoid any sliding effect on the surface of the plate. A solvent trap was used to limit solvent evaporation. Before measurements, the suspensions were pre-sheared at 20℃ at γ=60 s^{-1} for 1min followed by a recovery period of 10s. This pre-shear was indented to eliminate irreversible structures that can be formed during storage and suspension handling. This procedure allows to define a reference state of the suspension and to ensure a good reproducibility of rheological measurements.

Specific evolution of the rheological properties of the suspension are given in **Fig. 13**.

In the case of eflucimibe suspensions, the evolution of the shear rate is reasonably well described by the Herschel-Buckley model :

$$\frac{d\gamma}{dt} = 0 \quad for \quad \tau < \tau_c$$
$$\frac{d\gamma}{dt} > 0 \quad and \quad \tau = \tau_c + K\left(\frac{d\gamma}{dt}\right)^n \quad for \quad \tau > \tau_c \qquad (3)$$

where τ_c is the yield stress, K and n are the model factors.

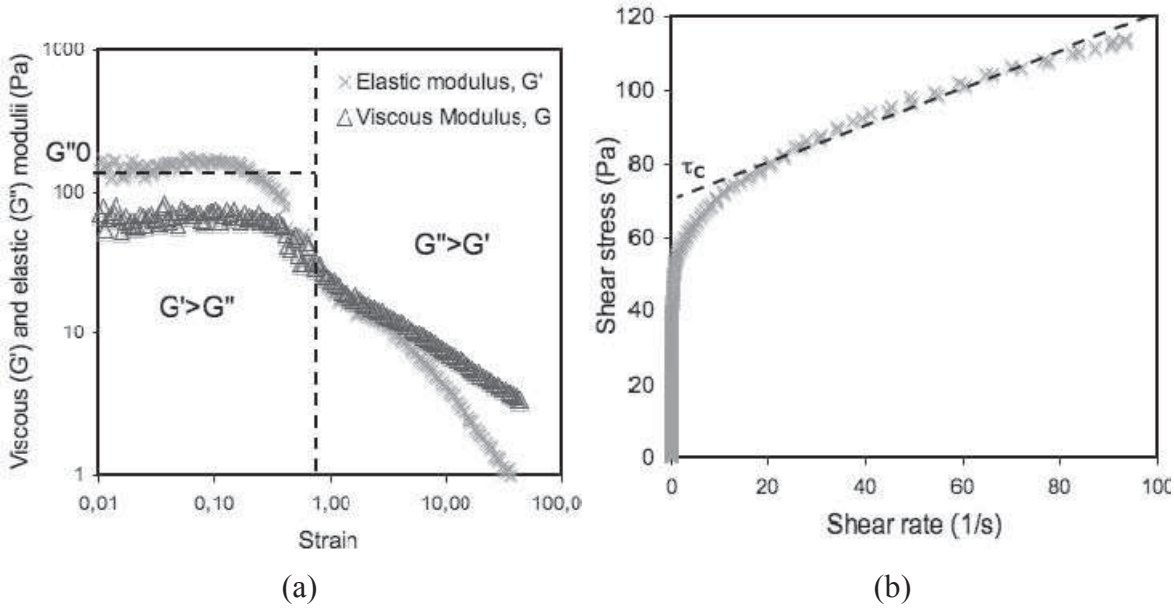

Fig. 14 Eflucimibe suspension rheology for a volume fraction of solids $\phi = 4\%$ (a) Oscillatory strain rheology (b) Simple shear rheology.

It was found that the rheological properties of the suspension are strongly dependent on solid volume fraction. **Table 3** summarizes the elastic modulii and yield stresses obtained for different concentrations.

This table shows that the yield stress and the elastic modulii increase when the solid volume fraction is raised. The low values of the elastic modulii and the yield stress suggest that the particle network is very weak. In addition, as observed during crystallization experiments, the yield stress, and thus the crystal network, disappear for a solid volume fraction lower than 2%. In addition, the visco-elastic properties of the suspension (i.e. τ_c and G'_0) are directly linked to the interparticle forces that build up the network. Theoretical development and experimental rheological studies (Brown 1988) suggest a power law dependence of the elastic modulus and the yield stress to the solid volume fraction. The exponent of the power law for the elastic modulus and the yield stress is linked to the aggregation mechanism and to the fractal dimension D_f by the following equations (Buscal et al. 1988):

$$G'_0 \propto \phi^n \rightarrow n = \frac{4.2}{3 - D_f} \tag{4}$$

$$\tau_c \propto \phi^m \rightarrow m = \frac{3}{3 - D_f} \tag{5}$$

The macroscopic elastic modulus (Eq. 4) is a function of both the spatial distribution of the aggregating particles, characterized by the fractal dimension D_f, and of the mechanical properties of the particles making of the network. The evolution of G'_0 versus ϕ is used to infer the mechanism by which the network was built. The m value was predicted to be 4.5 and 3.5 for a RLCA (reaction limited) and DLCA (diffusion limited) mechanisms, respectively.

Fitting of the power law on the experimental data are given in **Table 4**.

The results obtained for the elastic modulus scaling exponent m=3.4 is in good agreement with the theoretical values of a DLCA process. Moreover, the fractal dimension obtained by the two approaches are very close, Df = 1.7, suggesting a loose structure of the network.

Due to the weakness of the particles, it was impossible to sample the suspension and to analyze the particles by microscopy. As the shape and size of the primary particles are unknown, all the attempts made to model the particle organization in the network were unsuccessful. However, if a spherical shape can be supposed for the primary agglomerates, with a typical close packing of around 74%, it is found that, in order to reach a gelation threshold at 2%, the primary spherical particles have to be very porous with a void fraction around 70 to 80%. This observation is consistent with the fact that the particulate network is built with spherultic crystals (urchin-like crystals).

Table 3 Evolution of elastic modulii and yield stresses with the solid volume fraction of eflucimibe suspensions

Solid Volume Fraction, ϕ_s	Elastic Modulus, G_0' (Pa)	Yield Stress, τ_c (Pa)
0.019	-	-
0.022	164.2	7.0
0.028	420.5	9.1
0.035	744.4	17.2
0.041	1384.4	28.2
0.049	2366.1	37.5

Table 4 Results of the power law fitting of G'_0 and τ_c vs. ϕ

	Exponent	R^2	Df
G'_0	3.4 ± 0.2	0.996	1.7 ± 0.1
τ_c	2.2 ± 0.3	0.987	1.8 ± 0.1

5. Unconventional crystallization process : microfluidic tools

To get a better understanding of the process, crystallization experiments were performed in a microfluidic crystallizer. The "micro-crystallizer" consists in a 3m long crystallization channel with 220x100 μm cross sectional dimension. The microfluidic chip was designed in this study and built by Micronit company. In this system, droplets containing the organic solvent and solute are generated in water, each droplet acts as an independent crystallization container. The size of the droplet, and thus the crystallization volume can be finely tuned by altering the volume flow rate of each phase. Two phase flow microfluidic experiments, performed with five organic solvent in water, have enable to establish a correlation for predicting the droplet size from the physicochemical properties of the fluids and the volumetric flow rate of each phase. The obtained correlation (eq. 1) allows us to predict the droplet size with a precision around 10%.

$$\frac{L_{drop}}{d_{Channel}} = 1.5\left(\frac{Q_{disp}}{Q_{cont}}\right)^{0.2} Ca^{-0.2}\left(\frac{\mu_{disp}}{\mu_{cont}}\right)^{-0.2}\left(\frac{\rho_{disp}}{\rho_{cont}}\right)^{1/3} \quad (6)$$

In this study, as the dispersed and continuous phases are immiscible, a temperature gradient is applied to the chip to induce crystallization. Consequently, two temperatures regions, controlled by Peltier elements, have been defined: a heated zone (at the droplet generation) to avoid channels clogging, and a cooled region to induce nucleation.

The system is observed under microscope (Axio observer – Zeiss) and images are acquired using a sensitive CCD color camera (Sensicam PCO). The experimental setup is presented in **Fig. 15**.

To study the crystallization of eflucimibe in octanol, up to 2000 droplets were generated at 45℃ with a flow rate of 200µ l.h − 1 and 500µ l.h − 1 for octanol and water respectively. In this experiment, eflucimibe concentration was C^o=13.78mg.g $^{-1}$ and corresponds to its solubility in octanol at 40℃. Once the droplets are stored, the system is cooled down to either 20 or 5℃. The solubility of eflucimibe in octanol at 20 and 5 ℃ is 7.84 and 4,88 mg.g $^{-1}$ respectively.

The first crystals were obtained in the droplet for an induction time of 75min at 20℃ and 45min at 5℃. Photographs of the crystals obtained at 20 and 5℃ are given in **Fig. 16**.

At 20℃ (**Fig. 16a**), the spherulitic crystal tends to occupy all the space available in the droplet. If the droplet flows in the channel, the crystal blocks the flow inside the droplet. These observations, at the micrometric scale, can be linked to the rheological behavior of the suspension obtained in a stirred crystallizer. At 5℃, as shown in **Fig. 16b**, the crystals obtained are still spherulites but with a denser structure which might be easier to handle than in a crystallizer.

In that case, if the droplet flows inside the channel, the crystal moves freely inside the droplet.

In addition, nucleation kinetics and crystal growth kinetics have been determined in this system. Nucleation kinetics of eflucimibe in octanol has been deter-

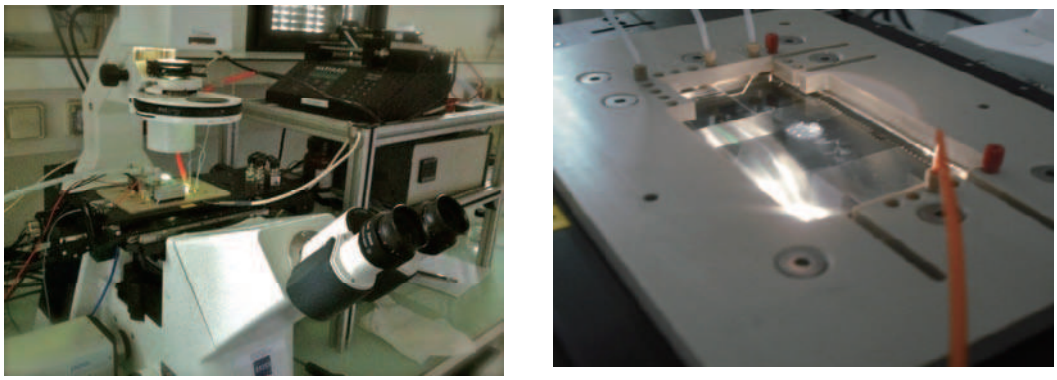

Fig. 15 (a) Experimental setup (b) microfluidic chip and housing.

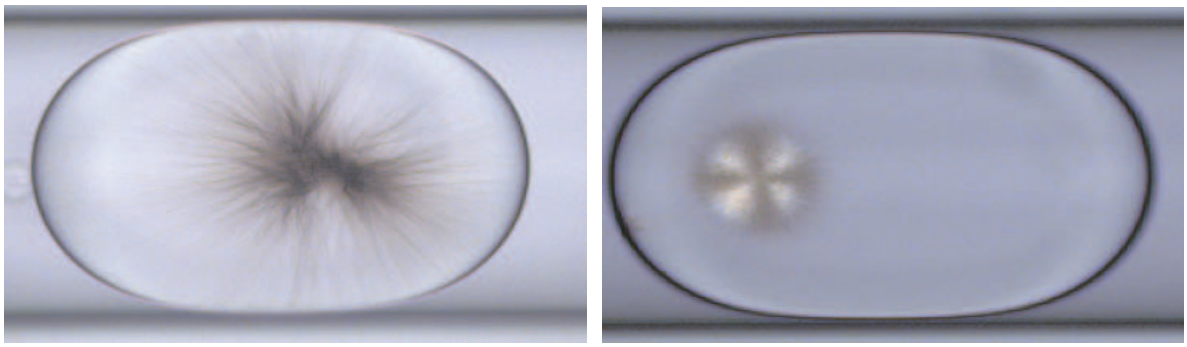

Fig. 16 Photographs of Eflucimibe crystals in octanol droplet under flow at (a) T=20℃ (b-c) T=5℃.

mined by counting the number of appearing crystals as a function of time in 2000 droplets generated at 45 ℃ and quenched to 20℃. The evolution of the number of uncrystallized droplets as a function of time is given in **Fig. 17a**. As shown in this figure, nucleation rate is not of first order and cannot be described by a classical Poisson distribution.

To describe the heterogeneous origin of the nucleation process, the model of Pound and Lamer (Pond and Lamer 1952) has been applied to the eflucimibe/octanol system. This approach provides a good fit of the experimental data and allows us to determine, in a single experiment, both heterogeneous and homogeneous nucleation rates. At low time scale, eflucimibe in droplets containing impurities will crystallize first and thus yields a rapid initial rate (i.e. heterogeneous nucleation rate). As these droplets are depleted, leaving only the droplets that are free of impurities, the rate will fall off, which allows to determine the homogeneous nucleation rate. The different nucleation rate thus obtained are given in **Table 5**.

Once a crystal is formed in a droplet, it is also possible to isolate droplets for measuring the crystal growth rate as a function of time. As an example, evolution of the crystal size in a droplet is plotted as a function of time in **Fig. 17b**. The radius scales with time as $t^{1/2}$, characteristic of diffusion-controlled growth.

In addition, using the crystal density determined by helium pycnometry (ρ_c=11200 kg/m^3), and assuming that the spherulites have a spherical shape, the void fraction of the crystals obtained at the end of the process (i.e the solution is at the thermodynamic equilibrium) can be calculated using the following expression:

$$\varepsilon = 1 - \frac{\rho_{spherulite}}{\rho_c} = 1 - \frac{(m_s^i - m_s^f)V_{spherulite}}{\rho_c} \quad (7)$$

Where m_s^i and m_s^f are respectively, the mass of eflucimibe in the solution before and after crystallization (ms = C^*V_{drop}), $V_{spherulite}$ is the spherulite volume ($V_{spherulite}=\pi d_3/6$). The void fraction obtained is 73%, which is in agreement with the void fraction previously supposed for the particles responsible of the crystallizer jamming.

This example clearly shows that microfluidic tools coupled with analytical techniques can be very useful to study, qualitatively and quantitatively, the crystallization process of complex structures under flow at a microscopic scale.

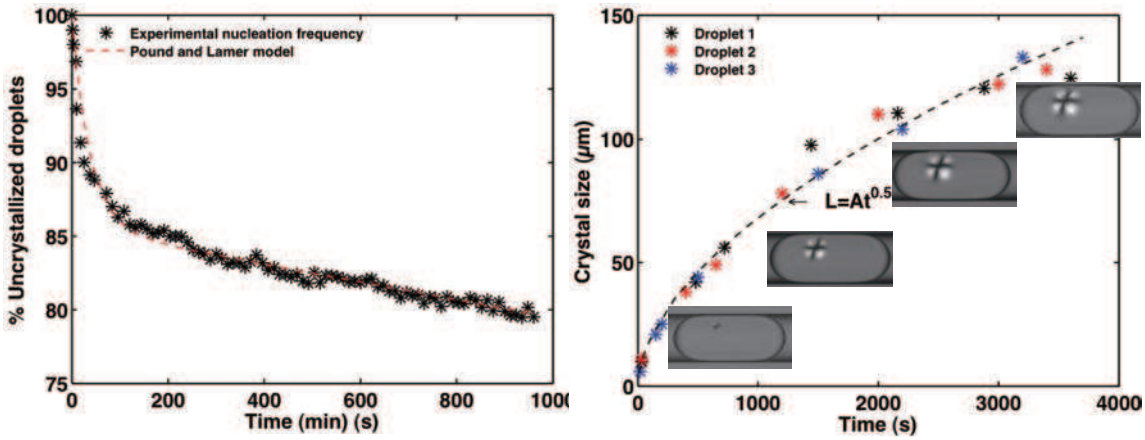

Fig. 17 Nucleation and growth of eflucimibe crystals in octanol droplet s(a) Nucleation rate : ratio of uncrystallized droplet vs. time and (b) growth kinetics of eflucimibe crystals (crystal size vs. time).

Table 5 Nucleation rate constant of the Pound and Lamer model

m*	J homogeneous (s^{-1})	J heterogeneous (s^{-1})
0.16	$1.23\ 10^{-6}$	$4.24\ 10^{-4}$

* m : mean number of impurities per droplet

Concluding remarks

In this study, we have shown that a multidisciplinary approach: from the molecules (solid state analysis, thermodynamics...) to the particles (rheology, microfluidic...) allows us to define the optimum operating conditions of a crystallization process to produce an API with a good yield, chemical purity and polymorphic purity. However, at this point, the suspensions obtained have poor handling properties such as flowability, filterability, bulk density... But, the results obtained at the micrometric scale show that eflucimibe crystallizes as spherulites under gentle hydrodynamic conditions (static or laminar flow in the microfluidic apparatus).

By taking into consideration all these observations, seeded crystallizations have been performed with low mixing intensity (N<50rpm). As shown in **Fig. 18**, the particles thus obtained are nearly spherical particles of polymorph A and present good flowability and filterability.

To conclude, we present in this paper a generic methodology for the crystallization of complex API: from molecular level studies to the crystallization process itself. In addition, we have shown how microfluidic tools, coupled with classical analysis or characterization techniques, can provide useful additional information about nucleation, growth and agglomeration of crystals.

Nomenclature

C^*	Saturation concentration	[mg/g]
C^o	Initial concentration	[mg/g]
Ca	Capillary number	[-]
Df	Fractal dimension	[-]
ΔG	Gibbs free energy difference	[J/mol]
G'	Elastic modulus	[Pa]
G''	Viscous modulus	[Pa]
J	Nucleation rate	[number/m^3/s]
Q	Volumetric flow rate	[m^3/s]
r	Nucleus radius	[m]
Ra	Molar fraction of ethanol in the solvent mixture on a solute free asis	
S	Supersaturation	[-]
T	Temperature	[℃]
V	Volume	[m^3]
w	Mass Fraction	[-]

Greek letters

μ	Viscosity	[Pa.s]
γ_{sl}	Solid-liquid interfacial tension	[mJ/m]
υ	Molcular volume	[m^3]
τ_c	Yield stress	[Pa]
ρ	Density	[Kg/m^3]
φ	Volume fraciton	[-]
ε	Void fraction	[-]

Subscripts

cont	Continus phase

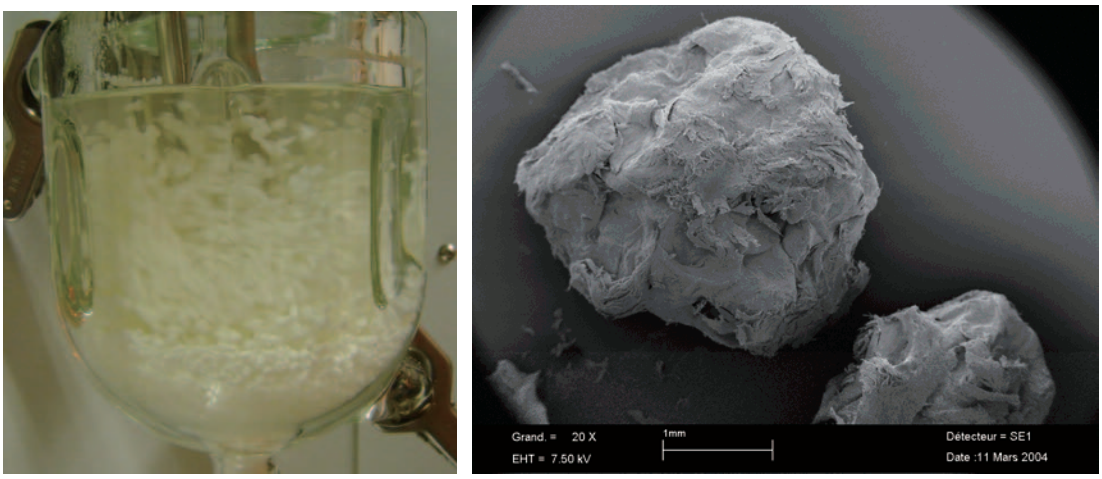

Fig. 18 Photograh of efflucimibe agglomerates (a) In the crystallizer (b) TEM images of agglomerates.

disp	Dispersed phase
crit	Critical
nucl	Nucleation
i	Component i

Acknowledgments

The author would like to thank Pierre Fabre Company for supporting this study and Richard Pena for his help in the solid state analysis.

References

Brown, W.D. and Ball, R.C. (1985): Computer simulation of chemically limited aggregation, J.Phys. A18, L517-L521

Buscall R., P. Mills, J.W. Goodwin, D.W. and Lawson, J. (1988): Scalling behavior of the rheology of aggregate networks formed from colloidal particles, J.Chem. Soc. Faraday Trans., 1, 84, pp.4249-4260.

Bustamante P, Navarro S, Romero S, Escalera B. (2002): Thermodynamic origin of the solubility profile of drugs showing one or two maxima against the polarity of aqueaous and non aqueous mixtures: Niflumic acid and caffeine, J PharmSci., 91, pp.874 883.

Domananska U. (1989): Solubility of acety-substitued naphtols in binary solvent mixtures, Fluid Phase Equilib., 55, pp.125-145.

Kashchiev, D. (2000): Nucleation, Basic Theory with Applications, Butterworth - Heinemann, Oxford.

Pound G. and La Mer V.K. (1952): Kinetics of Crystalline Nucleus Formation in Supercooled Liquid Tin, J. Am Chem. Soc., 74, pp.2323-2332.

Ribet, J. P., Pena, R., Chauvet, A., Patoiseau, J. F., Autin, J. M., Segonds, R., Basquin, M. and Autret, J. M. (2002): Polymorphisme cristallin de l'éflucimibe. Ann. Pharm. Fr., 60, pp.177-186.

Ulrich, J. and Strege, C. (2002): Some aspects of the importance of metastable zone width and nucleation in industrial crystallizers, J. Cryst. Growth, 237-239, pp.2130-2135.

Teychené, S., Autret, J. M., and Biscans, B. (2004): Crystalligation of Efluccimibe Drug in a Solvent Mixture, Effects of Process Conditions on Polymorphism Crystal Growth & Design 4 (5), pp.971 977.

Teychene, S., Autret, J. M., and Biscans, B. (2006): Determination of solubility profiles of eflucimibe polymorphs: Experimental and modeling, J. Pharm. Sci., 95 (4), pp.871-882.

Teychene, S. and Biscans, B. (2008): Nucleation kinetics of polymorphs: Induction period and interfacial energy measurements Crystal Growth & Des., 8 (4), pp.1133-1139.

Teychene, S., Autret, J. M. and; Biscans, B. (2006): Influence of crystallization conditions on rheology and microstructure of dense suspensions of crystals of eflucimibe, Chem. Eng. & Technol., 29 (2), pp.251-256.

Yu, L., Reutzel-Edens, S. M. and Mitchell, C. A. (2000): Crystallization and Polymorphism of Conformationally Flexible Molecules: Problems, Patterns, and Strategies, Org. Proc. Res. Dev., 4, pp.396 − 402.

Zettlemoyer, A. C. (1969): "Nucleation", Marcel-Dekker, New York,.

Author's short biography

S. Teychené

S. Teychené is an assistant professor in chemical engineering at the Laboratoire de Génie Chimique de Toulouse, Université de Toulouse (France). He received his engineer degree in chemical and environmental engineering in Institut National de Sciences Appliquées (INSA, Toulouse) in 2000, and his master degree in chemical engineering in 2001. He holds a Ph. D degree in chemical engineering from Toulouse university.
He joined the Laboratoire de Génie Chimique de Toulouse in 2006 in the team of Beatrice Biscans. His research interests are directed towards the thermodynamic and kinetics aspects of nucleation and phase transitions in the crystallization processes of organic coupounds.

Béatrice Biscans

Béatrice Biscans, Toulouse, France. Dr Béatrice Biscans obtained her degree in Chemical Engineering from the National Polytechnical Institute of Toulouse in 1982 and was awarded for her PhD in chemical and process engineering in 1985. After a post-doctoral position, she is working for the National Centre for Scientific Research (CNRS) since 1987 in the Chemical Engineering Laboratory of Toulouse (LGC). Her research is focused on Solid and Particles Processes. She is leading a group working on crystallization and formulation processes and nanoparticles production. She is today the Director of the Chemical Engineering Laboratory of Toulouse, as well as the President of the Working Party on Crystallization of the European Federation of Chemical Engineering and of the Working Party on Powders and Particles of the French Society of Chemical Engineering. She has an official position in CNRS as the French representative expert in Chemical Engineering.